Computing and Applied Sciences Impact (2025), 2(2): 16-44
ISSN: 3043-680X

Original Research

Synthesis, characterisation, *In Silico* analysis, and antimicrobial evaluation of mixed-ligand metal (II) complexes of quercetin-8-sulphonic acid and citric acid

Nzikahyel Simon [1*], Idongesit N. Ufot [1], Atim S. Johnson[1], Idongesit Anweting [1], Ekarika C. Johnson [2]

1. Department of Chemistry, University of Uyo, Uyo, Nigeria
2. Department of Pharmaceutical Chemistry, Faculty of Pharmacy, University of Uyo, Uyo, Nigeria

*****Corresponding author: Nzikahyel Simon (nzikahyelsimon@uniuyo.edu.ng)

Received: January 1, 2025; Revised: April 4, 2025; Accepted: April 20, 2025; Published: June 12, 2025

Abstract

A sulphonic derivative of quercetin and its four new mixed-ligand metal (II) complexes involving citric acid were synthesized, characterized, and tested against resistant bacteria and fungi. Characterization involved physicochemical techniques, elemental analysis, ultraviolet visible spectroscopy (Uv-Vis), Fourier transform infra-red spectroscopy (FTIR), Atomic absorption spectroscopy (AAS), Nuclear magnetic resonance (NMR) spectroscopy, and conductivity measurements. Elemental analysis results closely matched theoretical values. Conductivity studies indicated non-electrolytic behaviour and suggested octahedral geometry. Spectroscopic analyses confirmed complex formation, while NMR spectra identified substitution positions on the quercetin rings. Antimicrobial studies revealed that Manganese complex of quercetin-8-sulponic acid and citric acid [Mn(Q8SA)(CA)]Cl exhibited the highest antibacterial activity against *Pseudomonas aeruginosa* (35±1.2 mm at 100 µg/ml) compared to the sulphonic derivative (20±1.4 mm) and quercetin (16±1.5 mm). Cobalt complex of quercetin-8-sulphonic acid and citric acid [Co(Q8SA)(CA)]Cl showed the highest antifungal activity against *Aspergillus flavus* (25±1.3 mm at 50 µg/ml; 28±2.1 mm at 100 µg/ml) compared to the sulphonic derivative and quercetin (9±1.3 mm; 12±1.0 mm). Molecular docking revealed strong binding affinities (-11.0 to -8.0 kcal/mol among the complexes) surpassing quercetin and the derivative. However, biochemical parameters prediction disqualifies the complexes as potential drug candidates according to Lipinski's rule of 5. Antimicrobial effectiveness was concentration-dependent. The mixed-ligand metal (II) complexes exhibited superior chemical and biological properties compared to quercetin-8-sulphonic derivative, which in turn is better than standard quercetin *in vivo*, highlighting the potential of organic modification and metal coordination in addressing microbial resistance.

Keywords: Quercetin; Molecular docking; Antibacterial; Antifungal; Metal complexes

1. Introduction

Microorganisms, such as bacteria, viruses, or fungi, among others, can cause diseases either directly or indirectly. They are the main contributors to the high morbidity and death rates noted globally. The World Health Organisation (WHO) reports that 53 million people died worldwide in 2009, of which at least one-third were due to infectious diseases brought on by microorganisms [1]. Pneumonia, tuberculosis, dysentery, cholera, and AIDS are a few examples of these infections. Despite the fact that many drugs are produced to treat these illnesses, an increasing amount of antimicrobial resistance (AMR) is identified each year. In order to attain the Sustainable Development Goals (SDGs), WHO states that antimicrobial resistance is a global health problem that demands urgent multi-sectorial response [1].

AMR has therefore been listed as one of the top ten (10) worldwide public health hazards to humanity. The abuse and overuse of antibiotics, as well as genetic mutation in these organisms, are mostly to

blame for the high occurrence of AMR. Antibiotics are thus losing their efficacy as drug resistance grows internationally, making the treatment of illnesses more challenging. One of the mechanisms of organisms resistant to drugs involves being able to mimic the mode of action of the drugs metabolites [2]. The combination of two compounds through metal coordination is a good way of averting the organism's ability to decode the drugs [3]. Alternatively, it has been reported that many plant nutrients have therapeutic qualities. Due to its capacity to scavenge free radicals and consequent efficiency as an antioxidant, anticancer, antibiotic, and antiulcer, among other things, quercetin, a flavonoid (Fig. 1) is one of the most used and researched plant phytonutrients [4, 5].

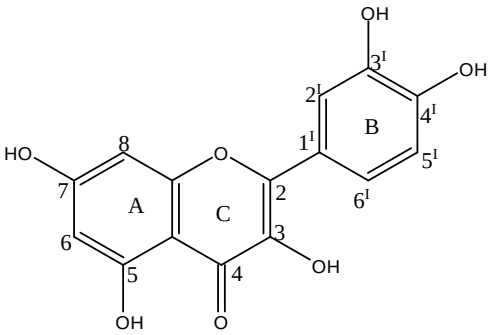

Figure 1: Structure of quercetin showing labelling of the rings and carbon atoms

According to Materska [6], quercetin mostly exists in bonded form with sugars, phenolic acids, and alcohols. Despite being abundant in products that are derived from plants, it is typically highly digested by biological processes, making it useless for reaching the cellular levels. Additionally, it has poor solubility in aqueous solution, making it a nonviable choice for drug formulation [7, 8]. Several strategies have been used in recent years to enhance this amazing phytonutrient's chemical and biological capabilities [9]. One of these is making use of its chelating and derivatization properties [10-12]. According to some reports, derivatised quercetin and its metal complexes have more beneficial characteristics than the original molecule [13-15, 12].

The first sulphonic derivatives of quercetin and morin with sulphonic group substitution at position 5^I were reported by Kopacz [16]. Subsequently, substitution at position 8 on the A ring was reported [17]. However, it was observed that sulphuric acid reacts with quercetin to yield these different products depending on the reaction conditions. In addition, some metal complexes of quercetin sulphonic acid derivatives have been reported [16, 18-20]. The derivatives formed complexes with p, d and f – electron metal ions in solution and in a solid state. The complexes were reported to be useful for spectrophotochemical and spectrofluorimetric determinations of some metal ions [21].

Citric acid has a strong antioxidant property. It is present in citrus fruits including oranges, limes, and lemons. It has been used as a weak acid that is naturally endowed with various health benefits for the treatment of conditions including kidney stones, skin infections, and blood purifier. Because it possesses anti-fungal, anti-virus, and antibacterial properties [22]. It is often used as a disinfectant and cleaning agent for homes.

To the best of our knowledge, the mixed ligand-metal (II) complexes of quercetin sulphonic acid and citric acid have not been reported. Hence, this work is focused on the synthesis and antimicrobial evaluation of some metal (II) complexes of quercetin-8-sulfonic acid with citric acid.

2. Materials and Methods

2.1 Materials

All the reagents and solvents were obtained from Sigma Aldrich, Germany, all of analytical grade and therefore were used without further purification. The main compounds used in the study were quercetin (Q) and citric acid (CA), while the metal salts were: cobalt (II) chloride hexahydrate, manganese (II) chloride, copper (II) chloride pentahydrate and zinc (II) chloride hexahydrate. The solvents utilized

include methanol, ethanol, concentrated sulphuric acid, dimethyl sulphoxide (DMSO), distilled water, and diethyl ether (DEE). Others are acetone and n-hexane.

Ultra-violet visible spectroscopy (Uv-Vis) spectra were obtained on a Uv-Vis spectrophotometer (Uv-Vis 2500, Techcomp, Hong Kong, China) using standard 1.00 cm quartz cells in DMSO as solvent. The infra-red (IR) spectra were recorded by using KBr pellets in the spectral range of 4000 – 400 cm^{-1} on a Cary 630 Fourier transform infra-red spectrophotometer, (Agilent, California, USA). The ^{1}H and ^{13}C NMR analyses of the derivatives were measured at 200 MHz in DMSO solvent using Bruker DPX-200 equipment (Bruker, Massachusetts, USA), while elemental analyses for the percentage composition of carbon, hydrogen, nitrogen and sulphur were obtained on a micro analyzer Perkin Elmer Series 11 Analyzer 2400 (PerkinElmer, Massachusetts, USA). An Alpha 4 atomic absorption spectrophotometer (Shimadzu, Kyoto, Japan) was employed to determine the amount of metals in the complexes. Also, the electrical conductivity measurements were carried out using a Hanna instrument conductivity meter, (Hanna Instruments, Rhode Island, USA), with a cell constant of 0.83, while the magnetic susceptibility measurements were obtained at room temperature with a Stuart instrument, Staffordshire, United Kingdom.

2.2 Synthesis of the derivatives

The sulphonic derivative of quercetin, namely: quercetin-8-sulphonic acid (Q8SA) was synthesised using the method earlier reported in literature [16]. A 24 cm^3 of concentrated sulphuric acid was added to 6 g of quercetin powder in a 250 cm^3 round-bottom flask. The reaction mixture was vigorously stirred for 2 h at 18 ℃ to obtain the 8-substituted derivative. The resulting precipitate was filtered and recrystallized in hot saturated water solution twice, then dried at room temperature.

2.3 Synthesis of the metal (II) complexes

The procedures previously reported [17, 23] were followed with some modifications. A 5 mmol of all the metal salts ($CuCl_2$•$2H_2O$ (0.6723 g), $CoCl_2$•$6H_2O$ (0.6490 g), $MnCl_2$•$4H_2O$ (0.6292 g), $ZnCl_2$•$4H_2O$ (0.9814 g)) were carefully calculated and weighed into separate beakers and were completely dissolved in 20 cm^3 of methanol. Also, 5 mmol of quercetin derivative [Q8SA (1.9116 g] was dissolved in the same quantity of methanol before being mixed with the metal salts' methanolic solutions (1:1 stoichiometric ratio) in each case and stirred for up to 30 minutes in a 250 mL round-bottom flask. Afterwards, a 5 mmol (0.96 g) citric acid dissolved in 20 cm^3 methanol solution was added and refluxed at 60 ℃ for 3 h in each case. The resulting mixture (which contained a 1:1:1 stoichiometric ratio of the derivative, metal salt and citric acid) was allowed to cool, then filtered. The precipitate formed was rinsed with 50 cm^3 methanol thrice before being washed with excess distilled deionized water. The product was dried over silica gel in a desiccator and used for further investigation. The reaction is summarized in Figure 2.

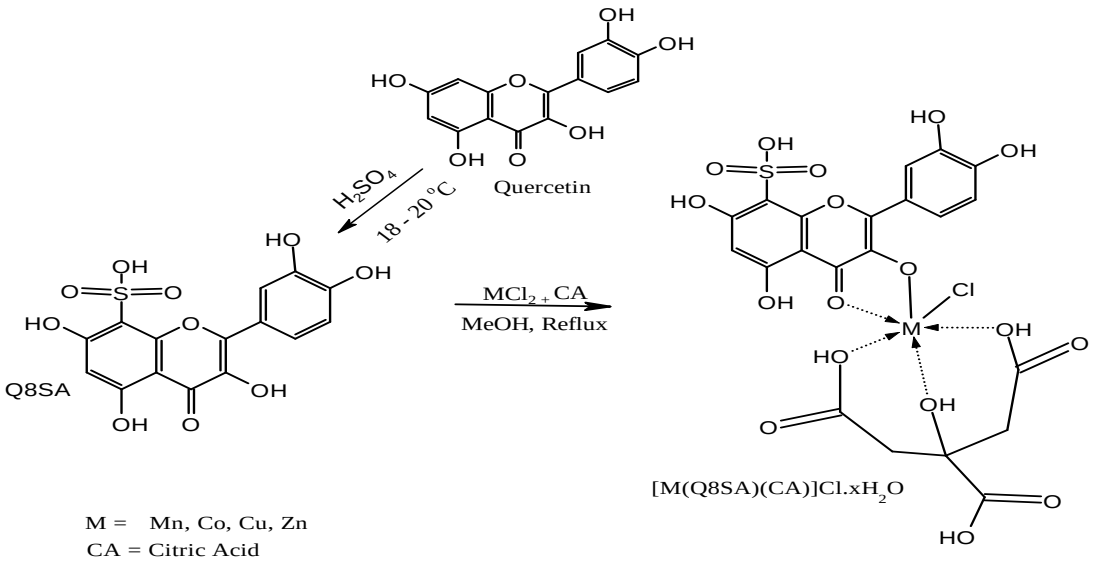

Figure 2: Schematic representation of the synthesis of the sulphonic-8-quercetin derivative and their mixed-ligand metal (II) complexes

2.4 Chemical measurements

Analysis of chemical elements (CHNS) was carried out using elemental analyser Perkin Elmer series 11 CHNS/O analyser 2400 (PerkinElmer, Massachusetts, USA). The melting point of the ligands and the complexes in this study were determined using the Stuart melting point apparatus. The colours of the metal complexes were observed under the microscope and confirmed by matching them with a colour chart. The conductivities of the ligands and complexes were measured in solvents in which the compounds were soluble using a Hanna instrument conductivity meter, with a cell constant of 0.83. All conductivity measurements were performed at room temperature using a 10^{-3} M solution of complex. Also, the refractive index of the compounds was measured using Stuart digital refractometer.

2.5 Instrumental analysis

The FTIR spectra of the derivatives and complexes were recorded using KBr pellets with a FTIR spectrophotometer. The metal analysis was carried out on an Alpha 4 atomic absorption spectrophotometer (Shimadzu, Kyoto, Japan). The electronic spectra of the complexes and derivative in solution of DMSO were run in the range 200 to 600 nm on a Uv-Vis spectrophotometer (Uv-Vis 2500, Techcomp, Hong Kong, China), whereas the ^{1}H and ^{13}C NMR analyses of quercetin and the derivative were measured at 200 MHz in DMSO solvent using Bruker DPX-200 equipment (Bruker, Massachusetts, USA) [24].

2.6 Antimicrobial screening

Antibacterial and antifungal activity of the new complexes and the ligands were carried out using the method reported in literature [25]. A seeded nutrient agar on which 0.5 mm diameter wells were punched and used on which the test organisms were inoculated. Different concentrations (50 µg/L and 100 µg/L) of the sterile filtered solutions of the compounds were made using DMSO as solvent and quercetin as control. A 0.1 ml of each concentration was applied into the wells and incubated at 37 ℃ for 24 h. The zone of inhibition were measured in triplicate based on the size of the zone of inhibition around the wells on the seeded nutrient agar. The bacteria species tested were: *Staphylococcus aureus* (*S.aureus*) *Echereshia coli (E.coli*), *Psuedomonas auroginosa* (*P. auroginosa*) and *kiebsiella pnuemonia (K. pnuemonia*). Also, the fungi include *Asperigillus flavus (A. flavus*), *Asperigilus niger* (*A. niger*), *Candida krusie* (*C. krusie)* and *Candida albican* (*C. albican*)

2.7 Molecular docking

Molecular docking is a computational technique in screening potential drug candidate by docking them on target macromolecules(protein) binding sites (26). The process involves the use of several software such as ChemSketch, Open babel, Autodock vina, Discovery studio and PyRx [27]. In this study, the Pyrx software was used for the docking process because of its simplicity and accuracy. The ligands (organic compounds) and their metal complexes were drawn using Chemsketch (Freeware 2023.1.1) and converted to the desired structure data format (sdf) with the help of Open babel program.

The target protein molecules were downloaded as 3D structures from Protein Data Bank website [28] and saved in pdb format. Discovery studio was used to visualise and prepare the target proteins by deleting water molecules, ligands present and all other chains except one to avoid complexity in the process. After these, polar hydrogens were added to the target molecule before being saved in pdb format. In the docking procedures, the target protein was opened in the PyRx and converted to pdbqt format. Then, the ligands were loaded using the open babel program embedded in PyRx, their energy minimised based on the default AutoDock Vina force field and then they were converted to pdbqt format before running the Autodock Vina program embedded in the PyRx software. The grid box centers and dimensions were set at maximum and hence generated automaticaaly by the program to coer the entire surface of the target protein [27]. The macromolecules used for the study are *S. aureus* penincilin binding protein -5M18 [29], *E. coli* membrane protein -5I5H [30]. *P. aeroginosa* hydrolase protein – 4A38 [31]. *A. niger* hydrolase protein – 1KS5 [32], *A. krusei* lipid binding protein – 5YB1 [33]. *K. pneumonia* transferase protien – 5KED [34], *A. flavus* gene regulation protein -8HBS [35], *Bacillus substilis* hydrolase protein- 4COT [36].

2.8 Biochemical properties prediction

Absorption, distribution, metabolism, excretion and toxicity evalations of the ligands were compared with that of their complexes using online software such as Swiss ADME (https://www.swissadme.ch). Protox-II (https://tox-new.charite.de/protox_II) and pkCSM (https://biosig.unimelb.edu.au/pkcsm) software were also used to predict use biochemical information regarding the compounds.

3. Results and Discussion

Quercitin-8-sulphonic acid was prepared by reacting concentrated H_2SO_4 with quercetin, thereafter, four (4) mixed-ligand metal(II) complexes were synthesised from the mixing of citirc acid, the different metal(II) ions with the newly prepared quercetin-8-sulponic acid (Figure 2). The resulting complexes have the following abbreviations: Copper complex of quercetin-8-sulphonic acid and citiric acid - [Cu(Q8SA)(CA)]Cl denoted as C1, Zinc complex of quercetin-8-sulphonic acid and citiric acid - [Zn(Q8SA)(CA)]Cl denoted as C2, Cobalt complex of quercetin-8-sulphonic acid and citiric acid - [Co(Q8SA)(CA)]Cl denoted as C3, and manganese complex of quercetin-8-sulphonic acid and citiric acid - [Mn(Q8SA)(CA)]Cl denoted as C4. The chemical and spectrophotochemical results of the analysis of the ligand and the complexes are shown in Table 1, while the elemental analysis is presented in Table 2.

All the compounds were soluble in DMSO. The changes in melting points and the colours observed in the complexes compared to those of quercetin and the derivative are evidence that new products were synthesised.. The molar conductance determinations show that the complexes C1–C4 are non-electrolytes as indicated in Table 1 [37]. The calculated elemental analysis results are in good agreement with those determined experimentally. The percentage of the metals in the mixtures was determined by AAS. Also, the magnetic susceptibility values suggest the presence of unpaired electrons in all the complexes except in Zn^{2+} complex as indicated in the results (Table 1). This shows that the anionic quercetin sulphonic acid ligand, chloride ions and citric acid are bonded to the metal (II) centres. Hence, an octahedral coordination is proposed for the complexes. The complexes also had different values of molecules of water of crystallisation. Chemical modification made to the quercetin structure by mixing it with sulphuric acid at 18 ^oC resulted in a derivative with improved chemical and biological activities [12, 14, 15]. This confirms earlier reports that substitution of the hydrophilic sulphonic group in positions 8 and 5^I on the quercetin structure greatly increases its aqueous solubility [38].

Table 1: Some analytical data of quercetin, its derivatives and metal (II) complexes

Compounds	Proposed formula	Colour	Yield (%)	Melting point (°C)	Electrical Conductivity (mΩ/cm/mol)	Magnetic susceptibility (BM)
Quercetin	$C_{15}H_{10}O_7$	Yellow	-	285	10.0	-
Q8SA	$C_{15}H_{10}O_{10}S$	Orange red	80.0	315	14.0	-
C1	$C_{21}H_{14}ClCuO_{17}S$	Green	58.0	375	15.0	1.86
C2	$C_{21}H_{14}ClO_{17}SZn$	Custom	68.0	349	16.0	-2.34
C3	$C_{21}H_{14}ClCoO_{17}S$	Brown	57.0	367	20.0	2.23
C4	$C_{21}H_{14}ClMnO_{17}S$	Deep brown	53.0	337	26.0	2.42

Table 2: Elemental composition of quercetin derivatives and the metal (II) complexes

Compounds	Analytically calculated (%)			Found (%)			
	C	H	S	C	H	S	M (AAS)
Q8SA	47.13	2.84	8.39	46.08	2.61	8.40	-
C1	37.68	2.11	4.79	37.84	2.21	4.70	9.49
C2	37.58	2.10	4.78	37.53	2.14	4.88	9.74
C3	37.14	2.12	4.82	37.09	2.10	4.89	8.87
C4	38.17	2,14	4.85	38.19	2.10	4.89	8.31

M(AAS) = AAS results for the composition of coordinating metals in the different complexes

3.1 The Uv-Vis spectroscopy

The Uv-Vis spectra of quercetin, derivatives and complexes C1–C4 were examined in DMSO solution of the compound. The Uv-Vis spectra of the derivative (Table 3, Appendix I and II) showed two absorption bands between 250 – 255 nm and 360 – 367 nm with different energies characteristic of quercetin [39]. Upon complexation with citric acid, the bands displayed bathochromic shifts as seen in Table 3. The increased absorbance in the range of 400–450 nm suggests a weak band which is connected with the d-d transition in the metal ions and a ligand-metal charge transfer [40].

The results suggest that the coordination of the derivatives with the metal ions occurred from the 3-OH and the 4-oxo groups close to ring B of the quercetin structure (Appendix I and II) [37]. The red shifts are also an indication of the increased conjugative effect observed when coordination reaction occurs to give a new ring in a metal complex (Fig. 2) [41, 42].

Table 3: Uv-Vis spectroscopy data

Compounds	Bands	Band I	Assignment	Band II	Assignment
Quercetin	376, 260	376	$\pi \rightarrow \pi^*$	260	$n \rightarrow \pi^*$
Q8SA	367, 253	367	$\pi \rightarrow \pi^*$	253	$n \rightarrow \pi^*$
C1	420, 254	420	d → d, LMCT	254	$n \rightarrow \pi^*$
C2	443, 254	443	d → d, LMCT	253	$n \rightarrow \pi^*$
C3	425, 256	425	d → d, LMCT	256	$n \rightarrow \pi^*$
C4	420, 252	420	d → d, LMCT	252	$n \rightarrow \pi^*$

LMCT = ligand metal charge transfer

3.2 Results of the FTIR analysis

The results of the IR analyses of the studied compounds are presented in Table 4. In the IR spectra of the derivatives, the O-H, C=O, C-OH and C-O-C stretching vibrations were observed (Appendix III). These values are also consistent with what has been reported earlier [42]. In the IR spectra of the complexes (Appendix IV -VI), the broad bands observed around 3420 – 3200 cm^{-1} are associated with the v(OH) vibrations of the water molecules. These values are also compatible with the elemental analysis data. The IR spectra of the complexes showed peaks related to ligands coordinated to a metal (II) ions. The C=O stretching mode of the derivatives usually occurs at around 1660 - 1654 cm^{-1} after complex formation. [43]. The shifts indicate the coordination of carbonyl oxygen with the metal ions. Moreover, the shift in C=O bond order when coordinated to metal ion along with 3-OH in complexes, may give rise to coupling of the vibrations of these two bands.

Also, the v(C-O-H) deformation mode observed between 1265 – 1250 cm^{-1} in the ligands are shifted to between 1367 – 1267 cm^{-1} in the complexes demonstrating an increase in the bond order which normally is observed when metal coordination involves the ortho-phenolic v(OH) group on the derivative B ring (Fig. 1) [43]. In addition, the occurrence of new bands in the region between 539 – 416 cm^{-1} attributed to a v(M-O) stretching vibration, indicates the formation of a metal complex. These bands are not seen on the spectra of the ligands [44].

3.3 NMR spectroscopy analysis

From the results, the ^{l}H and ^{13}C NMR spectra of quercetin and the derivative clearly showed changes resulting from shielding, deshielding and deprotonations that occurred on the main quercetin structure due to the derivatisation with sulphonic acid (Tables 5 and 6). There is an absence of a signal for H at the point of substitution on the quercetin. Also, the signal of the carbon at the point of substitution was affected. The ^{1}H and ^{13}C-NMR data show the downfield chemical shift in Q8SA (Appendix VII and VIII) as compared to free quercetin due to the substitution of the $–SO_2$ group. In Q8SA, the deprotonations of –18C resulted in a signal at 105.4 ppm because of the deshielding of the sulphonic group. Also, the appearance of signal upfield around 9.3 ppm for Q8SA at 26-OH, which is absent in the free quercetin, confirms substitution of the sulphonic functional group at that position [43].

Table 4: FTIR analysis results of quercetin (Q), the derivative (Q8SA) and complexes

Compounds	v(O-H) v(C-H) cm^{-1}	v(C=O) cm^{-1}	$v(C=C)^{+}$ cm^{-1}	Vasym (C=O) cm^{-1}	v(C-O) cm^{-1}	v(O-H) cm^{-1}	v(C-O) v(C-O-C) cm^{-1}	Vasym (SO_2) cm^{-1}	d(C-H) cm^{-1}	M-O cm^{-1}
Q	3408 3319	1886 1665	1613	1561 1522	1451	1383	1262		1015	
Q8SA	3419, 3126 ,2765, 2600	1660		1505	1456	1373	1250	1165	1034	
C1	3224, 2417	1652	1585	1545	1446	1364	1267	1162	1093	420
C2	3419, 2372	1654	1598	1521	1446	1425	1367	1168	1028	539
C3	3323	1654	1600	1580	1446	1335	1275	1163	1029	528
C4	3306	1654	1608	1530	1420	1369	1234	1192	1049	470

Table 5: ^{1}H NMR for the various protons on quercetin and the derivatives

Type of H	Quercetin signal (ppm)	Q8SA signal (ppm)
2 CH	-	8.60
8 CH	7.58	-
9 CH	6.85	-
11 CH	-	7.50
12 CH	7.71	-
13 OH	9.56	7.39
14 CH	-	6.79
16 CH	6.19	-
17 OH	-	6.97
18 CH	6.40	8.15
19 OH	-	12.25
20 OH	9.34	13.93
21 CH	9.72	-
22 OH	125.8	11.13
23 OH	10.81	-
26 OH	-	9.13

Note: (-) means no signal recorded. The labelling of the Protons is based on the setting of the equipment; hence the numbering is from C ring to A ring before B ring (Fig 1).

Table 6: ^{13}C NMR signals for the various carbons on quercetin and the derivatives

Type of H	Quercetin signal(ppm)	Q8SA signal (ppm)
1 C	147.4	145.0
2 C	136.1	136.0
3 C	177.5	176.0
4 C	103.3	107.6
5 C	157.7	151.6
7 C	122.7	123.1
8 CH	120.9	-
8 C	-	121.0
9 CH	116.1	116.0
9 C	-	-
10 C	148.8	148.8
11 C	145.6	145.6
12 CH	-	115.0
12 C	115.7	-
15 C	160.2	160.1
16 CH	99.3	100.5
17 C	165.0	153.0
18 CH	94.3	-
18 C	-	105.4

Note: (-) means no signal recorded. The labelling of the carbon atoms is based on the setting of the equipment, hence the numbering is from C ring to A ring before B ring (Fig. 1)

3.4 Results of antimicrobial screening

3.4.1 Antibacterial evaluations

The antibacterial activities of the ligands and complexes were evaluated based on the average size of the inhibition zone formed around the well on the seeded nutrient agar plate. The results of the antibacterial study using mixed-ligand complexes confirmed that the inhibition by the complexes are more effective compared to their respective ligands (Appendix IX). In comparing the inhibition ability of the complexes against each other (Figures 9–12), it is observed that for *S. aureus*, the highest inhibition activity was recorded with C3 (24±1.1 mm) at 100 µg/ml. For *E. coli*, C4 is the most active (28±1.1 mm). For *P. aeruginosa* and *K. pneumonia*, C4 displayed the highest inhibition. The inhibition seems to be concentration dependent, as observed in the most activity observed when 100 µg/ml is used compared to 50 µg/ml. The changes in inhibitory effects observed for the complexes may be attributed to the substitution effects during ligation. However, the improved activity observed with the complexes when compared to the ligands is due to the activation of the ligands by coordination reaction [45]. Also, there was no inhibitory activity on the solvent used in dissolving the compounds used as controls, and the results show there was no contribution of the activities from the solvent; hence, the result shows that the mixed-ligand metal complexes of quercetin sulphonic derivatives have more antibacterial inhibition properties [46].

3.4.2 Antifungal evaluations

Most of the metal (II) complexes showed higher antifungal inhibitory activities compared to their respective ligands (Appendix X). The comparative evaluations of these activities against the different organisms are shown in Figures 13–16. Generally, the antifungal activity of the complexes follows the trend: C3 > C1 > C2> C4. Though C4 displayed the least inhibition when compared to others generally, it shows the highest activity against *C. albicans* at 50 µg/ml (20±2.1 mm) and 100 µg/ml (25±1.2 mm). The metal complexes have higher activity against the tested fungi species compared to their corresponding ligands. This effect is attributed to the fact that metal coordination and chelating effect increase the chemical and biological activities of organic compounds [45, 46].

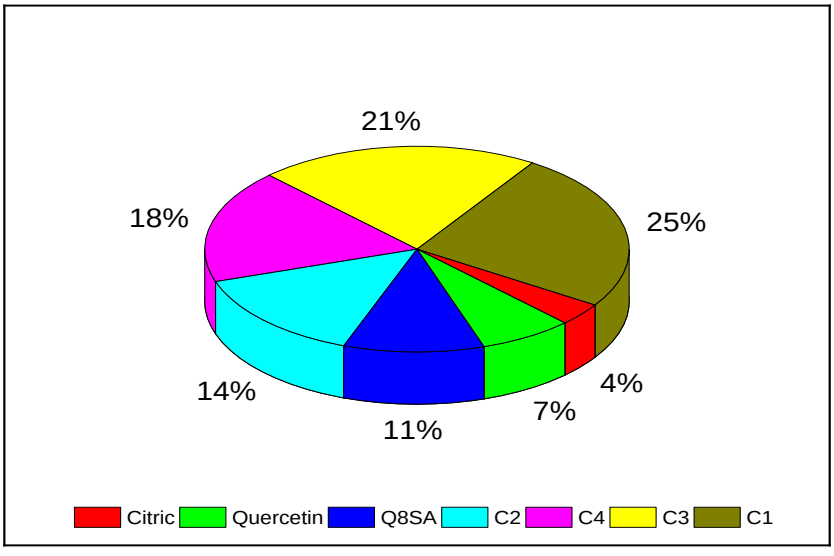

Figure 9: Comparison of the inhibition activity of the ligands and complexes at 50 µg/mL against *S. aureus*

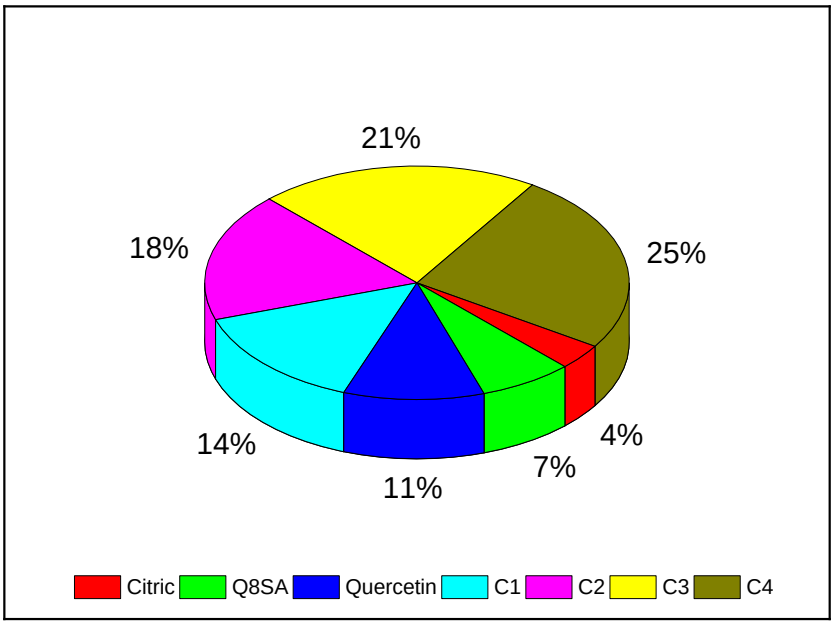

Figure 10: Comparison of the inhibition activity of the ligands and complexes at 100 µg/mL against *E. coli*

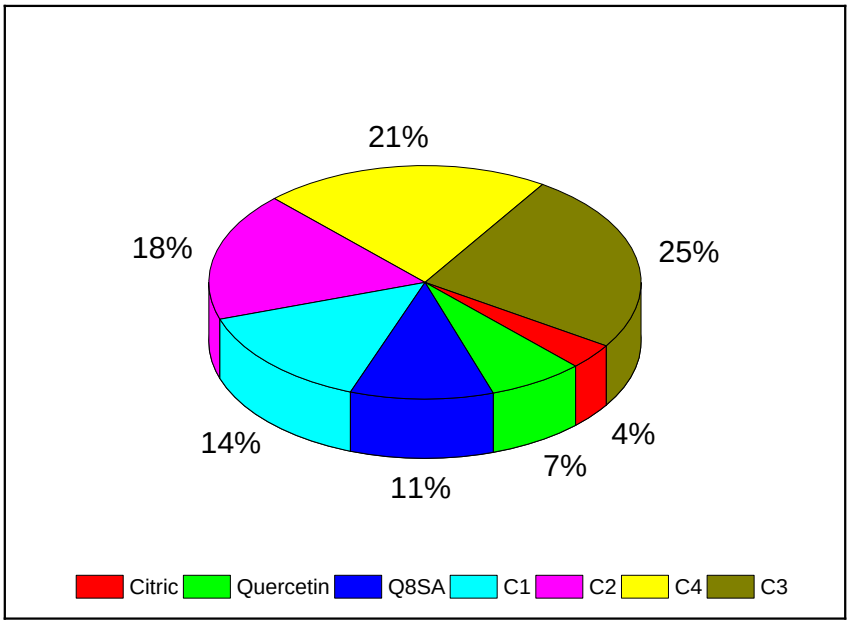

Figure 11: Comparison of the inhibition activity of the ligands and complexes at 50 µg/mL *A. aeruginosa*

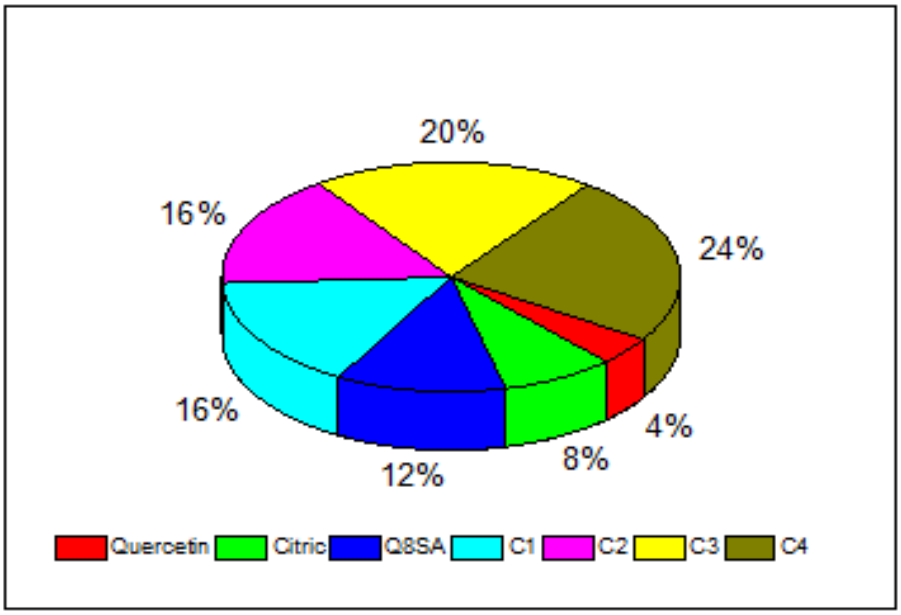

Figure 12: Comparison of the inhibition activity of the ligands and complexes at 50 µg/mL against *K. pneumonia*

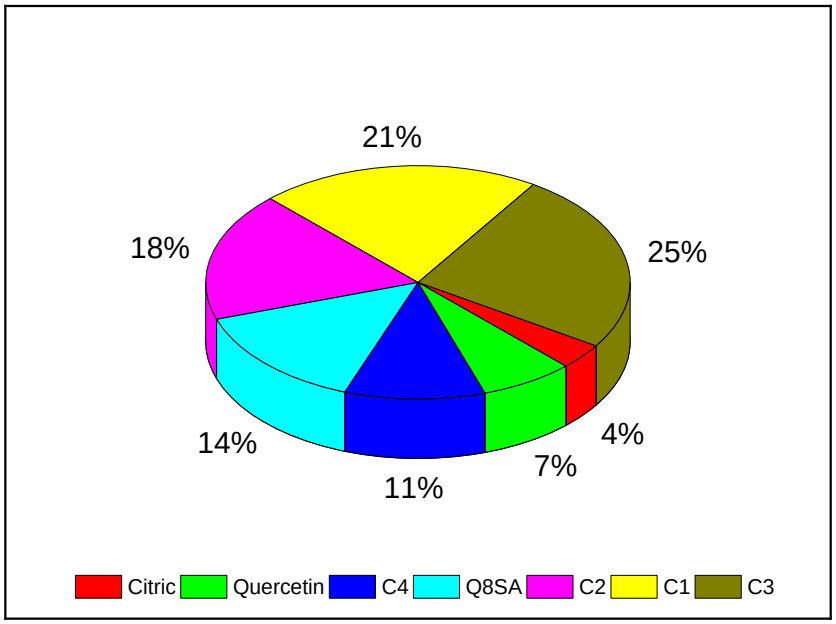

Figure 13: Comparison of the inhibition activity of the ligands and complexes at 50 µg/mL against *A. flavus*

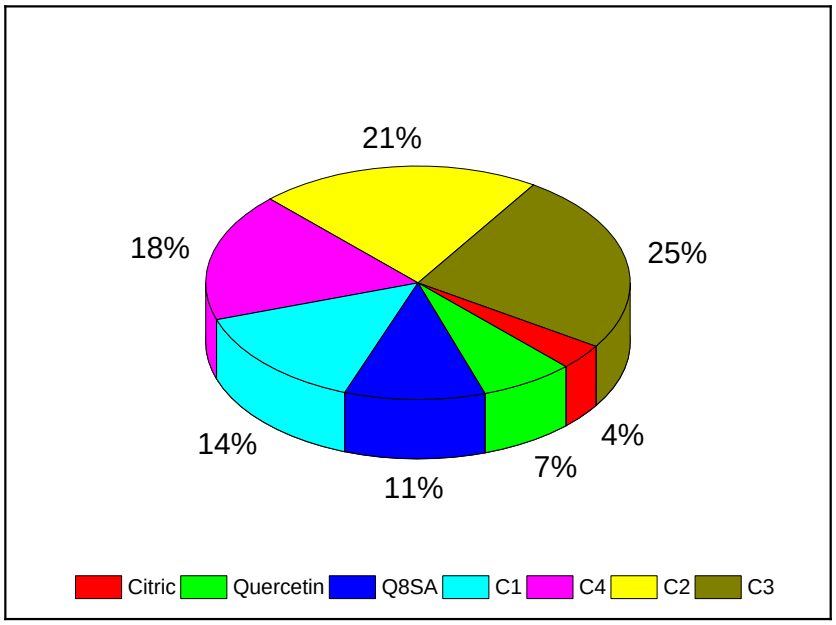

Figure 14: Comparison of the inhibition activity of the ligands and complexes at 100 µg/mL against *A. niger*

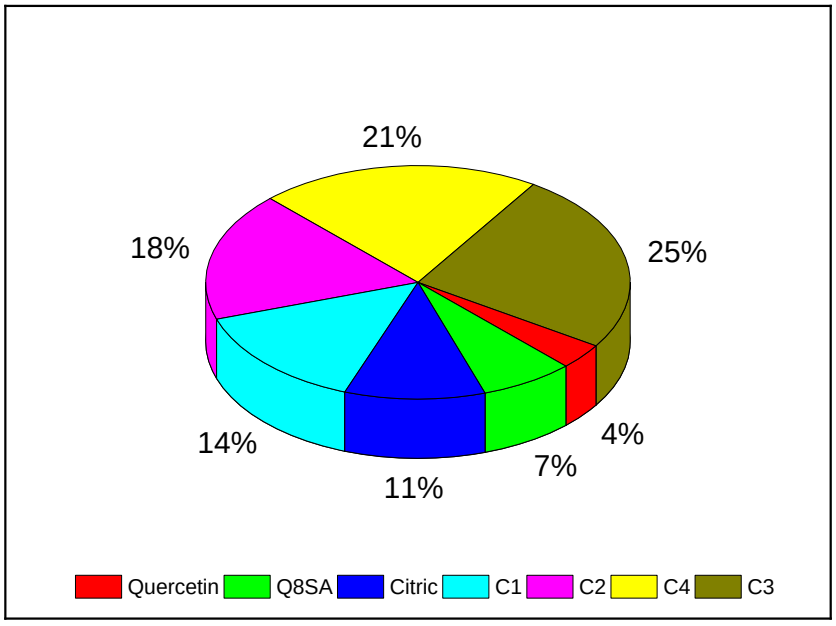

Figure 15: Comparison of the inhibition activity of the ligands and complexes at 100 µg/mL against *C. krusei*

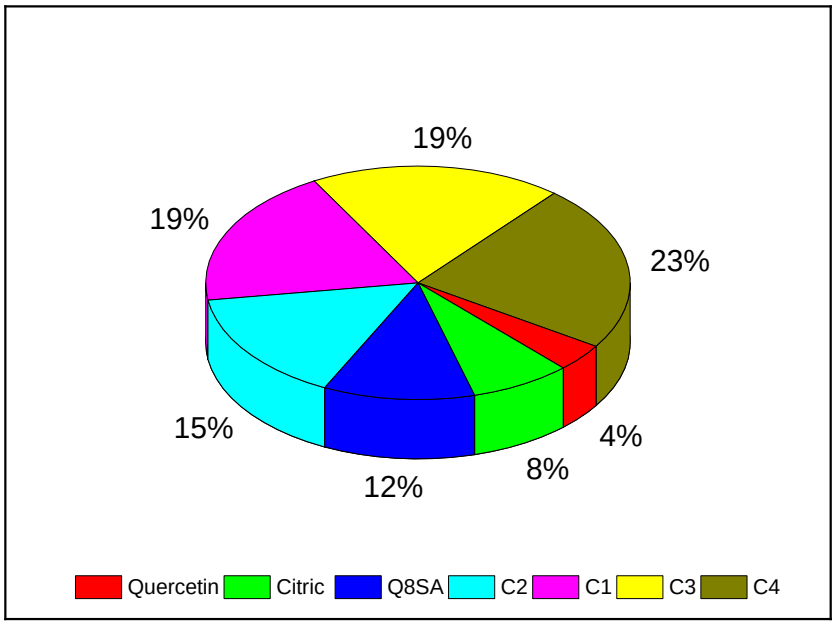

Figure 16: Comparison of the inhibition activity of the ligands and complexes at 50 µg/mL against *C. albicans*

3.5 Molecular docking results

Table 7 shows the most potent ligands with the highest binding affinity, and the various interactions that occurred between the ligands and the amino acid residues in the binding sites of the target protein macromolecules.

One of the striking observations from the results is that complexes involving Cu^{2+} do not come first in all the docking carried out. This might be related to the redox nature of Cu^{2+} when coordinated to quercetin in the biological systems [47]. It displays quite different dissociation mechanisms as compared to the other divalent ions such as Mn^{2+}, Co^{2+} and Zn^{2+}. This is partially due to the fact that Cu^{2+} has stronger oxidative activity and quercetin is easier to oxidize under acidic conditions [48]. Also, Cu^{2+} forms complexes with distorted octahedral or square planar geometries [49]. This might be less favourable for binding within the pockets of the target proteins [50]. It is also important to note that the active site of the receptor molecule is such a complex environment in which several interactions are possible [51]. This is observed in the different types of ligand–receptor interactions recorded (Figures 17 to 20). The complexes of quercetin-8-sulphonic acids bound more strongly to 5M18, 1KS5, 5YB1, 8HBS and 4COT, exhibiting better binding affinities compared to the ligands (Appendix XII–XIII)

From the above observations, it can be deduced that the binding affinity is highly affected by the nature of the ligands (their functionality), as well as the nature of the pocket of the binding site on the receptor molecule (the amino acid residues present). Hence, a better understanding of the function of a particular macromolecule, the amino acid residues involved in its interactions and the different functional groups in the ligands is crucial in selecting a ligand as a potential drug candidate for further investigation.

Table 7: Molecular docking results

Protein code	Description	Most potent ligand and its best binding affinity (kcal/mol)	RMSD value (A^o)	Number and length (A^o) of H bonds	Number of π bonds		
					π-π	π-alkyl	others
5M18	*S. aureus* (Penicillin binding protein)	C4 -9.3	50.7	3 (2.96, 2.13, 2.31)	1 (5.72)	4 (4.74, 4.54, 5.23, 4.81)	-
5I5H	*E. coli* (Membrane protein)	C3 -8.5	40.158	6 (2.04, 2.32, 2.70, 2.30, 2.92, 2.50)	2 (4.39, 5.30)	2 (5.51, 4.68)	
4A38	*P. aeruginosa* (Hydrolase)	C3 -10	2.101	5 (2.08, 2.30, 2.51, 2.47, 2.31)	1 (5.09)	2 (4.25, 5.20)	
1KS5	*A. niger* (hydrolase protein)	C2 -9.3	9.753	8 (2.51, 3.17, 2.91, 3.04, 3.17, 3.21, 2.01, 3.01)	5 (4.17, 3.50, 5.75, 5.49)	-	
5YB1	*C. krusei* (lipid binder protein)	C4 -10.5	3.983	2 (2.67, 2.28)	3 (5.45, 5.23, 3.79)	4 (4.94, 5.08, 4.98, 5.47)	2 (π-S 5.78. π-δ 3.94)
8HBS	*A. flavus* (gene regulation protein)	C4 -11	2.08	6 (2.93, 2.18, 2.12, 1.97, 2.11, 2.36)	4 (5.53, 6.52, 4.05, 4.47)	1 (6.49)	1 (C-H 3.19)
4COT	*C. albicans* (transferase protein)	C2 -8.9	7.436	5 (2.65, 2.30, 2.06, 1.96, 2.96)	3 (π-C 3.73, π-anion 3.49, 4.55)	-	1 (C-H 3.35)

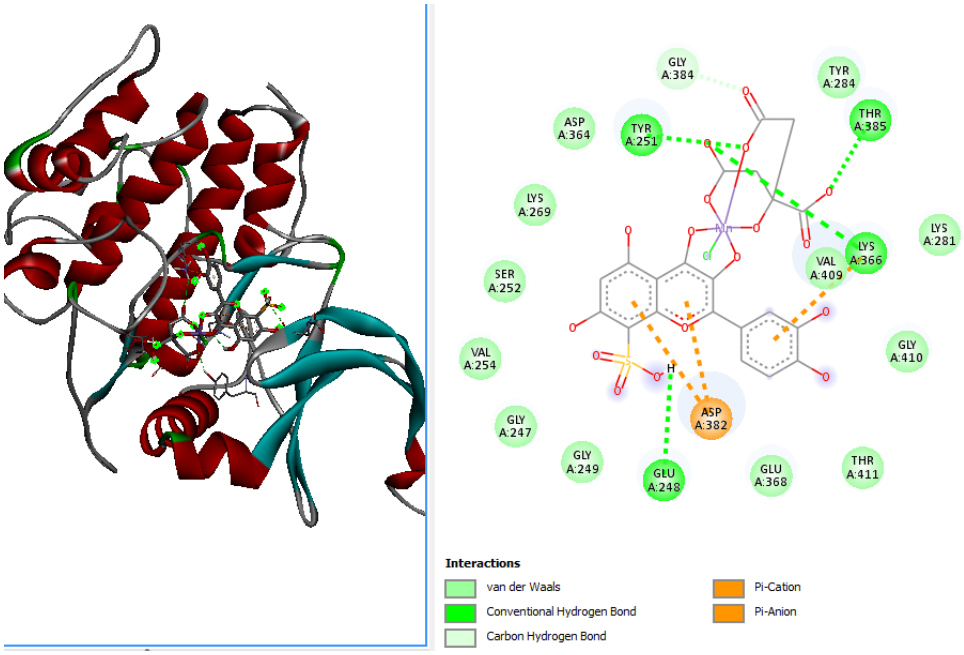

Figure 17: 3D and 2D representation of C2 interactions with 4COT

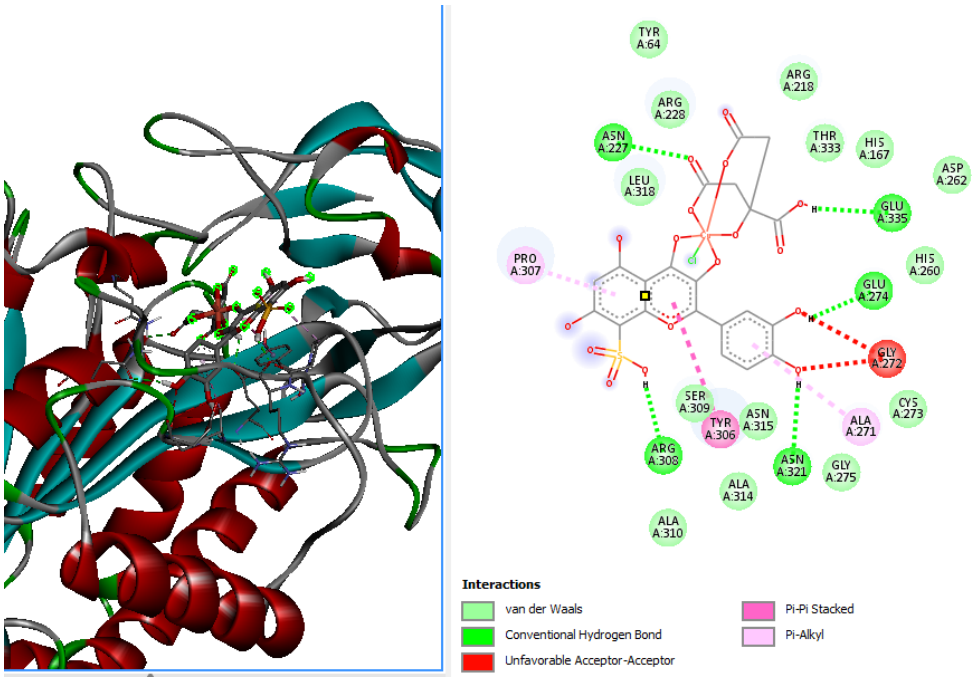

Figure 18: 3D and 2D representation of C3 interactions with 4A38

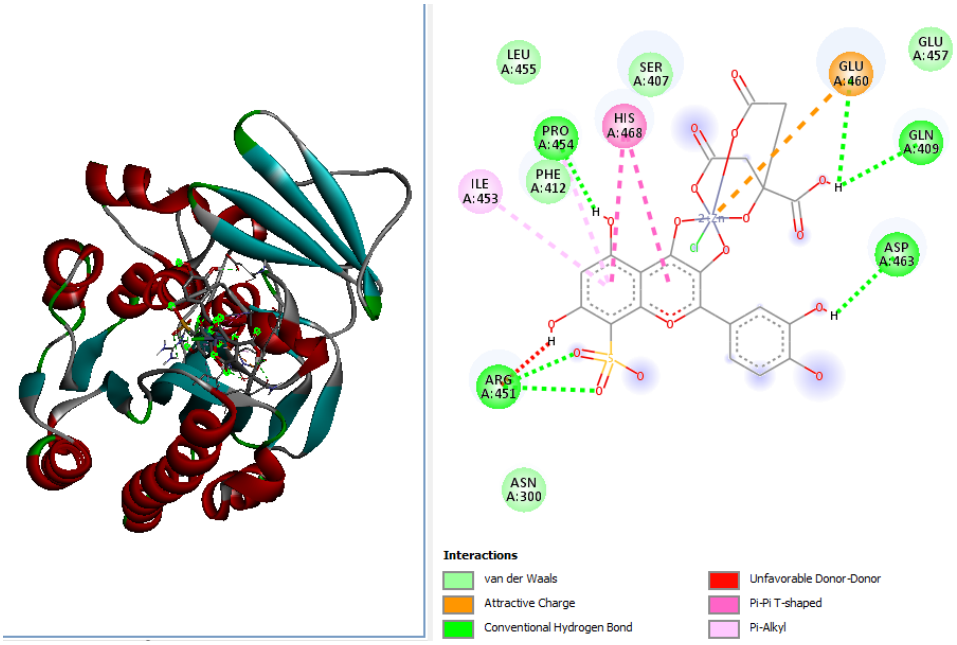

Figure 19: 3D and 2D representation of C3 interactions with 5I5H

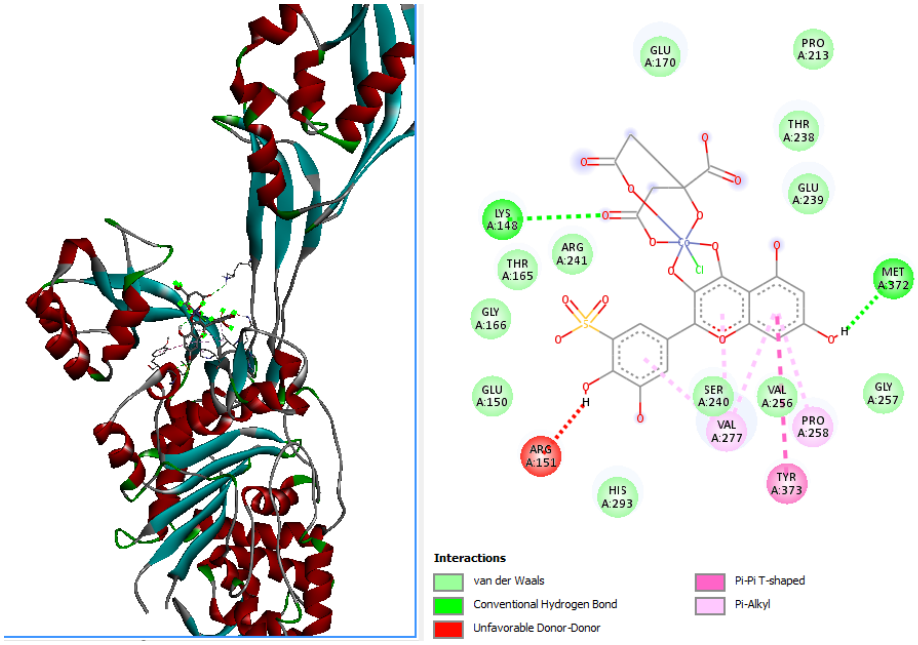

Figure 20: 3D and 2D representation of C4 interactions with 5M18

3.6 Predictions of some biochemical properties of the ligands and their complexes

The results of the absorption, distribution, metabolism, and excretion (ADMET) parameters of the studied ligands are recorded in Appendix XIV. This could not be performed on the complexes due to the limitations of the applied software. Several changes are observed, especially in absorption and distribution between the pure quercetin and the derivative, which indicate modifications due to the substitution of the sulphonic group to the quercetin ring. Though quercetin shows better absorption than Q8SA (74.63% versus 41.04%), Q8SA is predicted to be slightly more soluble than quercetin hence should have a higher volume of distribution and fraction unbound. Also, quercetin shows high drug interaction risks, while Q8SA has a higher clearance rate than quercetin. Appendix XV indicates the toxicity data for the ligands. This prediction suggests that both quercetin and Q8SA will be toxic while Q8SA shows higher toxicity compared to quercetin. Appendix XVI shows some other useful biochemical parameters of both the ligands and their metal (II) complexes. As indicated, quercetin has the best oral absorption, but with high toxicity (LD_{50} = 159 mg/kg), the derivative and the metal complexes show poor bioavailability due to a high number of H-bond acceptors. Moreover, while C2 shows slightly lower toxicity, C3 show the lowest skin permeability.

The variations in the data obtained suggest changes attributed to the introduction of the $–SO_2$ functional group, the presence of a metal ion and the coordination of the co-ligand, which alters the chemical properties of the parent compounds. Quercetin is shown to be highly metabolized, while the derivatives and the complexes are not. Though the data presented are derived from several models, they indicate further investigation. However, the coordination of the metal ions with the co-ligands to the derivatives has so increased their molecular weight above 500 g/mol, which disqualifies them for application as drug compounds according to the Lipinski's rule of 5 [52]. Nevertheless, these strategies of modification could improve the chemical and biological properties of organic compounds making them more suitable as a candidate for drug development. This is reasonable because it could make these compounds more available at the cellular level, as well as being more potent against multidrug-resistant organisms.

4. Conclusion

Improvement of the chemical and antimicrobial properties of quercetin has been achieved through derivatisation and metal coordination. Since more hydrophilic compounds show higher antibacterial activity than the less hydrophilic, it was expected that the sulphonic derivatives will be better inhibitors of bacterial growth than the parent compounds and this has been confirmed through the many data that are presented in this work. Hence, the new compounds synthesised through mixed-ligand metal (II) coordination reaction using citric acid as co-ligand, have some better increased beneficial properties compared to quercetin and its sulphonic derivatives apart from the increased molecular weight and high toxicity. However, this strategy shows promising outcomes that can be harnessed to improve the potency of the currently resisted drug compounds provided the Lipinski's rule of 5 is obeyed

Acknowledgements
None

Funding
None

Conflict of Interests
There is no conflict of interest between the authors.

Author Contributions
All the authors read and made inputs to the manuscript. Idongesit Ufot conducted the molecular docking in addition to the experimental measurements.

References

[1] World Health Organization (WHO), "*Diabetes"*. [Online Resource]. Available at: https://www.who.int/news-room/fact-sheets/detail/diabetes. [Accessed: October 14, 2022].

[2] N. Ka-Zemipour, S. Nazifi, M. H. Poor, Z. Esmailnezhad, R. E. Najafabadi, and A. Esmaeili, "Hepatotoxicity and nephrotoxicity of quercetin, iron oxide nanoparticles, and quercetin conjugated with nanoparticles in rats," *Comparative Clinical Pathology*, 27(4), 1621–1628, **2018**.

[3] C. Serafim, M. E. Araruna, E. A. Júnior, M. Diniz, C. Hiruma-Lima, and L. Batista, "A review of the role of flavonoids in peptic ulcer (2010–2020)," *Molecules*, 25(22), 5431, **2020**.

[4] M. Materska, "Quercetin and its derivatives: chemical structure and bioactivity—a review," *Polish Journal of Food and Nutrition Sciences*, 58(4), 407–413, **2008.**

[5] H. Pool, S. Mendoza, H. Xiao, and D. J. McClements, "Encapsulation and release of hydrophobic bioactive components in nano emulsion-based delivery systems: Impact of physical form on quercetin bio accessibility," *Food & Function*, 4(1), 162–174, **2013**.

[6] B. Alsofyani, R. S. Alayli, M. S. Alayli, T. S. Alkhaldi, G. H. Altalhi, and M. A. Rahman, "Solubility enhancement of a model drug quercetin by nanotechnology based formulation approach" *Biological Sciences*, 3(4), 509–515, **2023**.

[7] E. S. Attar, V. H. Chaudhari, C. G. Deokar, and P. V. Devarajan, "Nano drug delivery strategies for an oral bioenhanced quercetin formulation," *European Journal of Drug Metabolism and Pharmacokinetics*, 48(3), 495–514, **2023**.

[8] Z.-H. Shi, N.-G. Li, Y.-P. Tang, Q.-P. Shi, H. Tang, W. Li, X. Zhang, H.-A. Fu, and J.-A. Duan, "Biological evaluation and SAR analysis of O-methylated analogs of quercetin as inhibitors of cancer cell proliferation," *Drug Development Research*, 75(7), 455–462, **2014**.

[9] N. S. Ahmad, M. Farman, M. H. Najmi, K. B. Mian, and A. Hasan, "Pharmacological basis for use of *Pistacia integerrima* leaves in hyperuricemia and gout," *Journal of Ethnopharmacology*, 117(3), 478–482, **2008**.

[10] M. A. Ghareeb, A. Z. Zayan, F. H. Shari, and A. M. Sayed, "Unveiling the potential of quercetin: Chemistry, health benefits, toxicity, and cutting-edge advances," in *Quercetin - Effects on Human Health*, J. Osredkar (Editor), IntechOpen, London, United Kingdom, **2024**, pp. 123–145.

[11] Y. Liu and M. Guo, "Studies on transition metal-quercetin complexes using electrospray ionization tandem mass spectroscopy," *Molecules*, 20(5), 8583–8394, **2015**.

[12] T. S. De-Castilho, T. B. Matias, K. P. Nicolini, and J. Nicolini, "Study of interaction between metal ions and quercetin," *Food Science and Human Wellness*, 7(3): 215–219, **2018**.

[13] M. Khater, D. Ravishankar, F. Greco, and H. Osborn, "Metal complexes of flavonoids: their synthesis, characterisation, and enhanced antioxidant and anticancer activities," *Future Medicinal Chemistry*, 11(21), 2845–2867, **2019**.

[14] M. Kopacz, "Quercetin and morin sulfonates as analytical reagents," *Journal of Analytical Chemistry*, 58(3), 225–229, **2003**.

[15] M. Kopacz and A. Kuznier, "Complexes of cadmium (II), mercury (II) and lead (II) with quercetin-5-sulphonic acid (QSA)," *Polish Journal of Chemistry*, 77(12), 1777–1786, **2003**.

[16] G. Dehghan and Z. Khoshkan, "Tin (II) quercetin complex; synthesis, spectral characterisation and antioxidant activity," *Food Chemistry*, 131(2), 422–426, **2012**.

[17] S. M. R. Al-Jabban, X. Zhang, G. Chen, E. A. Mekuria, L. H. Rakotondraibe, and Q.-H. Chen, "Synthesis and anti-proliferative effects of quercetin derivatives," *Natural Product Communications*, 10(12), 2113–2118, **2015**.

[18] M. A. Lutoshkin, I. A. Petro, A. S. Kazachenko, B. N. Kuznetson, and V. A. Levdansky, "Complexation of rare earth metals by quercetin and quercetin-5-sulphonic acid in acidic aqueous solution," *Main Group Chemistry*, 17(1), 17–25, **2018**.

[19] P. Godlenska, J. Hamza, E. Kucharska, P. Solarz, and S. Roszak, "Optical and magnetic properties of lanthanide (III) complexes with quercetin-5-sulphonic acid in the solid state and silica glass," *Journal of Molecular Structure*, 1219, 128504, **2020**.

[20] C. Luciano, B. Max, J. D. Catravas, and P. E. Marik, "Quercetin and vitamin C: An experimental, synergistic therapy for the prevention and treatment of SARS-CoV-2 related disease (COVID-19)," *Frontiers in Immunology*, 11, 1451, **2020**.

[21] A. Pękal, M. Biesaga, and K. Pyrzynska, "Interaction of quercetin with copper ions: complexation, oxidation and reactivity towards radicals," *Biometals*, 24(1), 41–49, **2011**.

[22] E. Elīuz, "Antimicrobial activity of citric acid against *Escherichia coli*, *Staphylococcus aureus* and *Candida albicans* as a sanitizer agent," *Eurasian Journal of Forest Science*, 8(3), 295–301, **2020**.

[23] A. Bravo and J. R. Anacona, "Metal complexes of the flavonoid quercetin: antibacterial properties," *Transition Metal Chemistry*, 26, 20–23, **2001**.

[24] A. Ahmedova, K. Paradowska, I. Wawer, ^{1}H, ^{13}C MAS NMR and DFT GIAO study of quercetin and its complex with Al(III) in solid state. *Journal of Inorganic Biochemistry*, 110, 27–35, **2012**.

[25] A. Raza, X. Xu, L. Xia, C. Xia, J. Tang, and Z. Ouyang, "Quercetin-iron complex: synthesis, characterization, antioxidant, DNA binding, DNA cleavage, and antibacterial activity studies," *Journal of Fluorescence*, 26(6), 2023–2031, **2016**.

[26] B. Kumar, J. Devi, A. Dubey, and M. Kumar, "Exploration of newly synthesized transition metal (II) complexes for infectious diseases," *Future Medicinal Chemistry*, 16(20), 2087–2105, **2024**.

[27] O. Trott, and A. J. Olson, "AutoDock Vina: Improving the speed and accuracy of docking with a new scoring function, efficient optimization, and multithreading," *Journal of Computational Chemistry*, 31(2), 455–461, **2010**.

[28] H. M. Berman, J. Westbrook, Z. Feng, G. Gilliland, T. N. Bhat, H. Weissig, I. N. Shindyalov, and P. E. Bourne, "The protein data bank," *Nucleic Acids Research*, 28(1), 235–242, **2000**.

[29] K. V. Mahasenan, P. Molina, R. T. Bouley, A. Batuecas, Y. Y. Lee, J. M. Lastochkin, C. Fisher, A. W. Chowdhury, M. R. Hermoso, B. Shoichet, S. Mobashery, and M. C. Llarrull, "Structure and function of an L,D-transpeptidase from Mycobacterium tuberculosis that rescues PBP-deficient mutants," *Journal of the American Chemical Society*, 139, 2102–2110, **2017**.

[30] H. Dong, Q. Xiang, Y. Gu, Z. Wang, N. G. Paterson, P. J. Stansfeld, C. He, Y. Zhang, W. Wang, and C. Dong, "Structural basis for outer membrane lipopolysaccharide insertion," *Nature*, 511, 52–56, **2014**.

[31] A. Otero, M. Rodriguez De La Vega, S. M. Tanco, J. Lorenzo, F. X. Aviles, and D. Reverter, "Crystal structure of a novel human cystatin family protein (CSTP1)," *FASEB Journal*, 26, 3754–3764, **2012**.

[32] S. Khademi, D. Zhang, S. M. Swanson, A. Wartenberg, K. Witte, and E. F. Meyer, "Determination of the structure of an endoglucanase from *Aspergillus niger* and its mode of inhibition by palladium chloride," *Acta Crystallographica Section D: Biological Crystallography*, 58 (4): 660–667, **2002**.

[33] K. Zheng, Q. Wu, C. Wang, W. Tan, and W. Mei, "Ruthenium(II) complexes as potential apoptosis inducers in chemotherapy," *Anticancer Agents in Medicinal Chemistry*, 17 (1): 29–39, **2017**.

[34] M. A. Schumacher, "5KED: Structural insights into the regulation of multidrug recognition complex BmrR," *RCSB Protein Data Bank*, 2016. Available: https://www.rcsb.org/structure/5KED. Retrieved March, 22, **2022**.

[35] Y. Wang, R. Lin, M. Liu, S. Wang, H. Chen, W. Zeng, X. Nie, and S. Wang, "N-myristoyltransferase, a potential antifungal candidate drug-target for *Aspergillus flavus*," *Microbiology Spectrum*, 11, e0421222, **2023**.

[36] C. E. McVey, M. J. Ferreira, B. Correia, S. Lahiri, D. De Sanctis, M. A. Carrondo, P. F. Lindley, I. De Sa Nogueira, C. M. Soares, and I. Bento, "The importance of the Abn2 calcium cluster in the endo-1,5-arabinanase activity from *Bacillus subtilis*," *Journal of Biological Inorganic Chemistry*, 19, 505–513, **2014**.

[37] H. M. Gençkal, M. Erkisa, P. Alper, T. Eren, B. Coban, E. Yavaş, D. Gozuacik, S. Yelekci, and M. Ariöz, "Mixed ligand complexes of Co(II), Ni(II) and Cu(II) with quercetin and diimine ligands: synthesis, characterization, anti-cancer and anti-oxidant activity," *Journal of Biological Inorganic Chemistry*, 25: 161–177, **2020**.

[38] L. Zhang, D. Lin, X. Sun, U. Curth, C. Drosten, L. Sauerhering, S. Becker, K. Rox, and R. Hilgenfeld, "Crystal structure of SARS-CoV-2 main protease provides a basis for design of improved α-ketoamide inhibitors," *Science*, 368, 409–411, **2020**.

[39] M. M. Rafeeq "Molecular docking analysis of phytochemicals with estrogen receptor alpha," *Bioinformation*. 18(8):697–702. **2022**.

[40] E. Woznicka, M. Kopacz, M. Umbreit, and J. Kłos, "New complexes of La(III), Ce(III), Pr(III), Nd(III), Sm(III), Eu(III) and Gd(III) ions with morin," *Journal of Inorganic Biochemistry*, 101, (5), 774–782, **2007**.

[41] S. V. Jovanovic, S. Steenken, M. Tosic, B. Marjanovic, and M. G. Simic, "Flavonoids as antioxidants," *Journal of the American Chemical Society*, 116, 4846–4851, **1994**.

[42] E. Woźnicka, E. Pieniążek, L. Zapała, Ł. Byczyński, I. Trojnar, and M. Kopacz, "New sulfonic derivatives of quercetin as complexing reagents: Synthesis, spectral, and thermal characterization," *Journal of Thermal Analysis and Calorimetry*, 120 (1), 351–361, **2015**.

[43] N. Mahar, S. Memon, A. A. Hulio, Q. K. Panhwar, and I. Mahar, "Synthesis and antioxidant activity of mixed ligand complex of quercetin and aspartic acid with cobalt (II)," *Journal of Medicinal Chemistry*, 8, 253–258, **2018**.

[44] B. A. Lakshmi, J. Y. Bae, J. H. An, and S. Kim, "Nanoclusters prepared from ruthenium(II) and quercetin for fluorometric detection of cobalt(II), and a method for screening their anticancer drug activity," *Microchimica Acta*, 186, 539, **2019**.

[45] J. Porkodi and N. Raman, " Synthesis, characterization and biological screening studies of mixed ligand complexes using flavonoids as precursors," *Applied Organometallic Chemistry.* 32(2), e4030, **2017**.

[46] N. Raman, L. Mitu, A. Sakthivel, and M. S. S. Pandi, "Studies on DNA cleavage and antimicrobial screening of transition metal complexes of 4-aminoantipyrine derivatives of N_2O_2 type," *Journal of the Iranian Chemical Society*, 6, 738–748, **2009**.

[47] W. M. B. Da-Silva, O. P. Solange, D. R. A. Daniela, J. E. S. A. Jane, F. E. A. M. Francisco, F. C. O. S. Fransica, J. S. Jacilene, E. S. M. Emmanuel, and S. M. M. Selene, "Synthesis of quercetin-metal complexes, in vitro and in silico anticholinesterase and antioxidant evaluation, and in vivo toxicological and anxiolytic activities," *Neurotoxicity Research*, 37, 893–903, **2020**.

[48] M. Kim, S. C. Jee, M.-K. Shin, D.-H. Han, K.-B. Bu, S.-C. Lee, B.-Y. Jang, and J. S. Sung, "Quercetin and isorhamnetin reduce benzo[a]pyrene-induced genotoxicity by inducing RAD51 expression through downregulation of miR−34a," *International Journal of Molecular Sciences*, 23, 13125, **2022**.

[49] A. A. Sharfalddin, A. H. Emwas, M. Jaremko, and M. A. Hussien, "Transition metal complexes of 6-mercaptopurine: characterization, theoretical calculation, DNA-binding, molecular docking, and anticancer activity," *Applied Organometallic Chemistry*, 35(1), e6041, **2021**.

[50] L. Cao, B. Coventry, I. Goreshnik, R. Huang, J. S. Adams, L. J. L. Boyken, J. B. Ueda, J. A. Fallas, N. P. Sameera, L. Ovchinnikov, A. R. Hosseinzadeh, S. Chen, J. Roel-Touris, C. M. Eastman, E. Tolman, S. Gopal, J. K. Jensen, S. Sood, K. J. Whitehead, K. E. Bohn, A. R. Kephart, K. M. Bakota, C. J. Hallinan, J. H. Kim, Y. Yu, M. A. M. Remis, S. S. Hekstra, A. W. Senior, J. Jumper, R. Evans, J. Meiler, D. S. Marks, J. D. Bendall, T. E. Mallajosyula, N. P. King, and D. Baker, "Design of protein-binding proteins from the target structure alone," *Nature*, 605, 551–560, **2022**.

[51] A. Dubey, S. Dotolo, P. Ramteke, A. Facchiano, and A. Marabotti, "Searching for chymase inhibitors among chamomile compounds using a computational-based approach," *Biomolecules*, 9: 5, **2019**.

[52] C. A. Lipinski, F. Lombardo, B. W. Dominy, and P. J. Feeney, "Experimental and computational approaches to estimate solubility and permeability in drug discovery and development settings," *Advanced Drug Delivery Reviews*, 23, 3–26, **1997**.

SUPPLEMENTARY INFORMATION

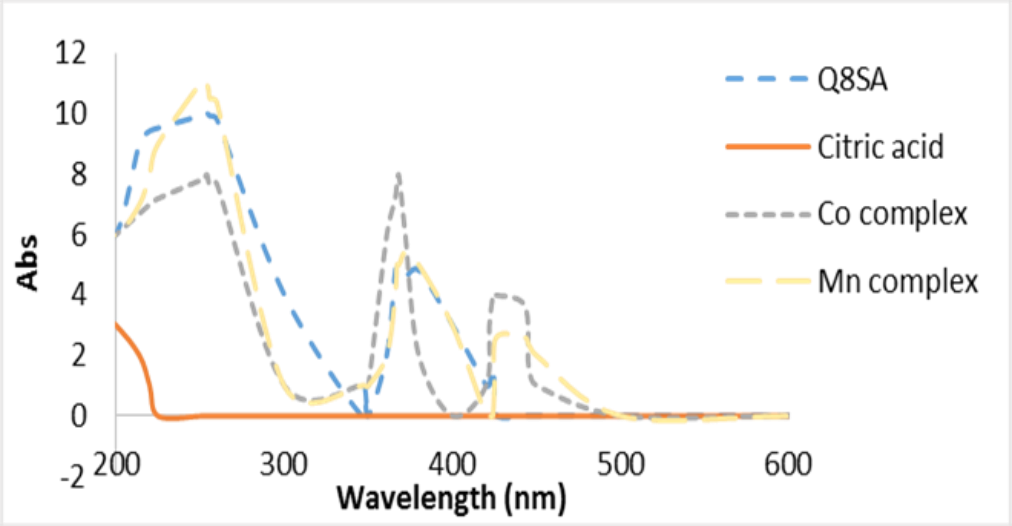

Appendix I: Stacked Uv-Vis spectra of Q8SA, citric acid, Co and Mn complexes

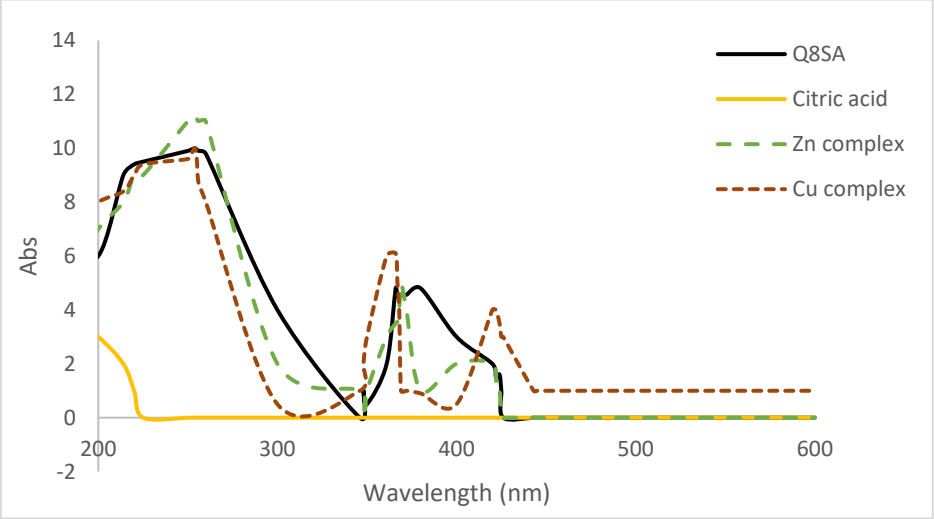

Appendix II: Stacked Uv-Vis spectra of Q8SA, citric acid and Zn and Cu complexes

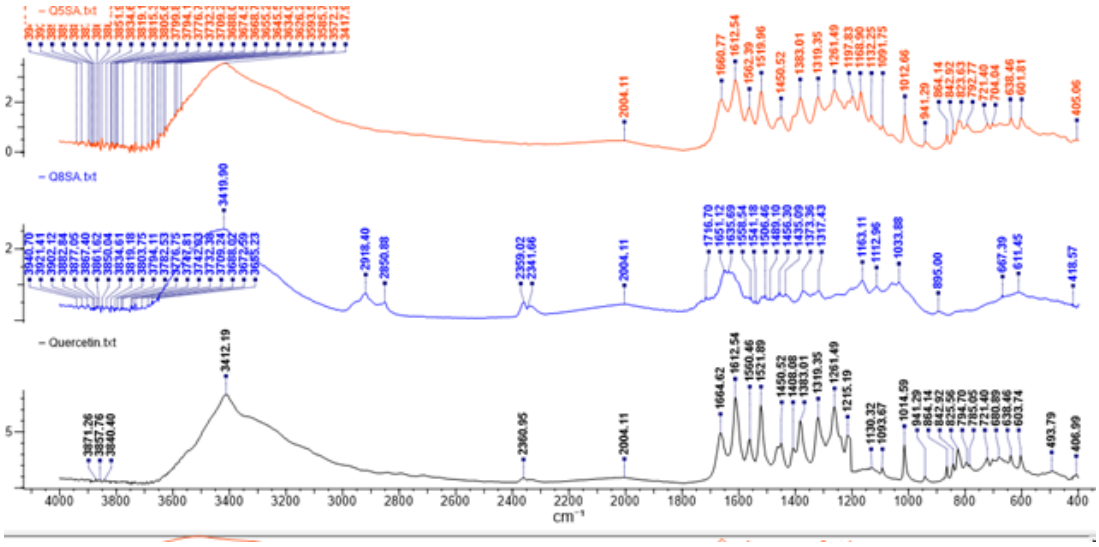

Appendix III: Stacked FTIR spectra of quercetin and the derivatives

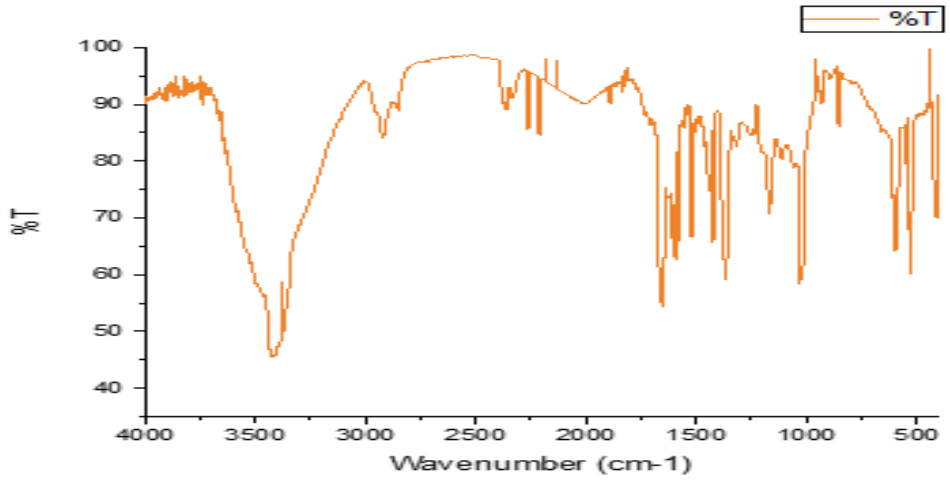

Appendix IV: FTIR spectrum of C3

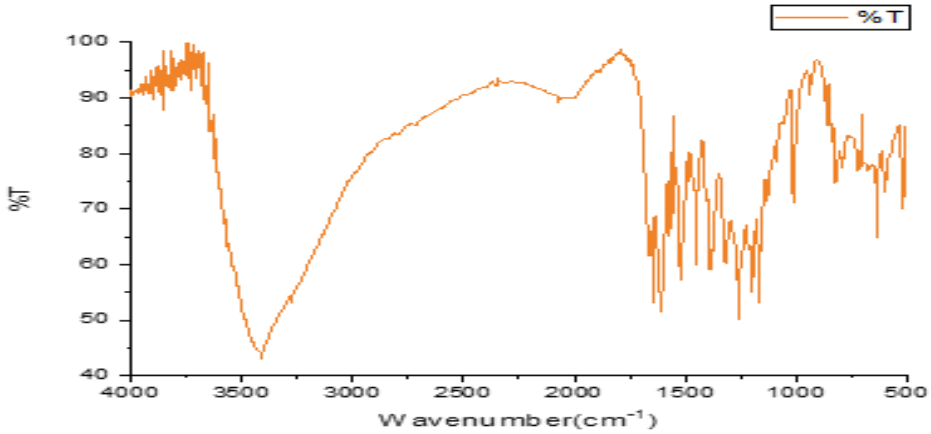

Appendix V: FTIR spectrum of C1

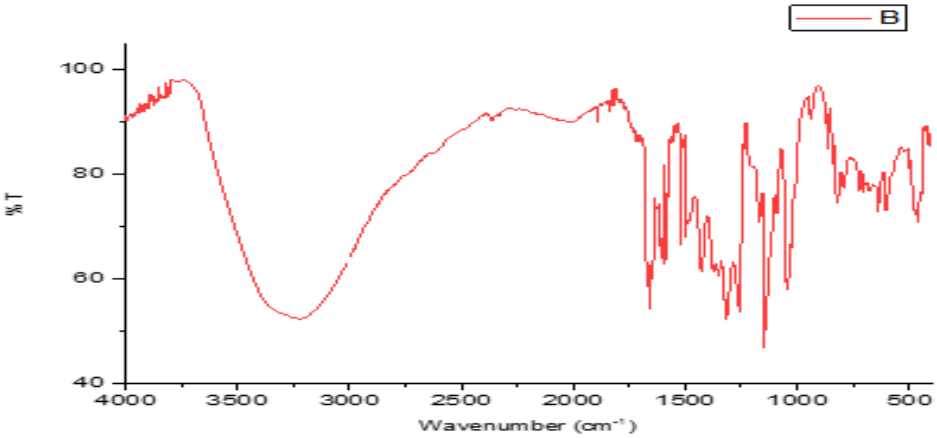

Appendix VI: FTIR spectrum of C4

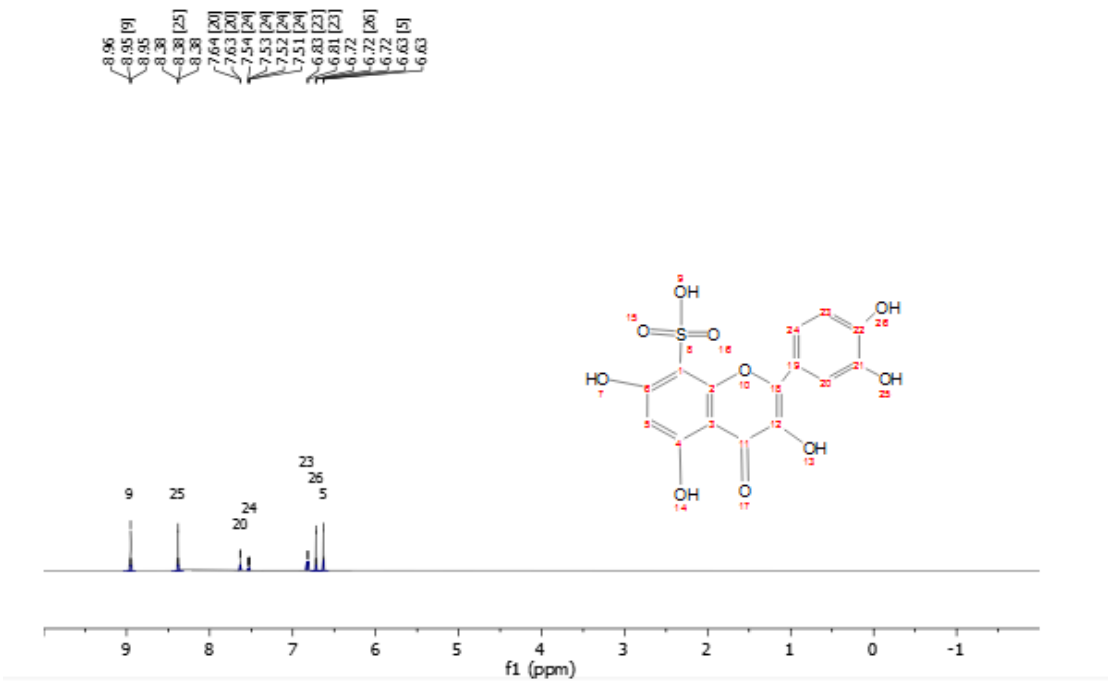

Appendix VII: [1]H NMR spectrum of Q8SA

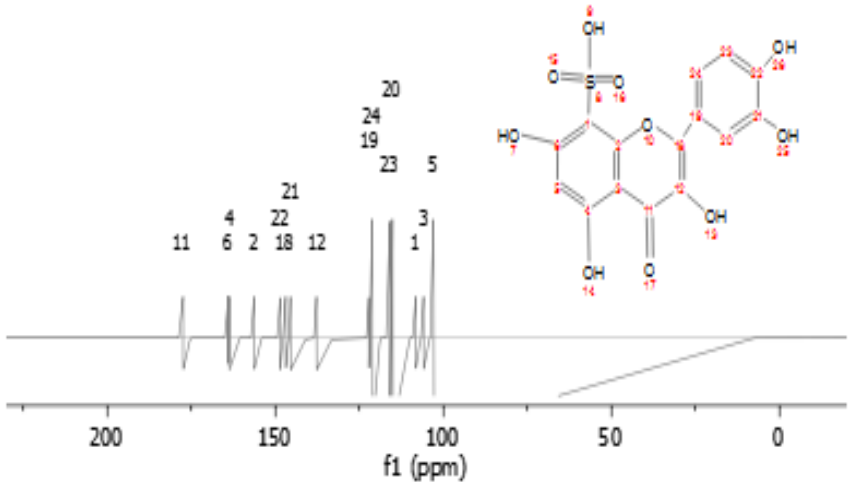

Appendix VIII: [13]C NMR spectrum of Q8SA

Appendix IX: Results of antibacterial evaluation

Compound	*S. aureus*		*E. coli*		*P. aeruginosa*		*K. pneumonia*	
	Zone of Inhibition (mm)							
	50 µg/ml	100 µg/ml	50 µg/ml	100 µg/ml	50 µg/ml	100 µg/ml	50 µg/ml	100 µg/ml
Quercetin	10±0.3	19±6.7	12±1.1	14±1.2	16±1.8	16±1.5	12±1.5	12±1.2
Citric acid	2±2.1	2±2.1	10±1.1	12±1.3	11±1.2	12±1.4	9±1.2	9±2.1
Q8SA	12±1.1	13±1.1	13±1.3	13±1.6	16±1.0	20±1.4	10±2.6	13±1.6
C1	16±1.1	22±1.2	20±1.1	15±1.1	17±1.1	18±1.3	15±2.1	19±1.4
C2	14±2.1	22±1.0	27±1.1	17±1.1	22±1.1	26±1.3	15±2.1	17±2.4
C3	15±1.2	24±1.1	20±1.1	22±1.4	25±1.4	26±1.1	16±1.5	20±1.2
C4	14±2.8	15±1.1	16±2.4	28±1.1	22±1.8	35±1.2	24±2.1	25±1.6

Appendix X: Results of antifungal evaluation

Compound	*A. flavus*		*A. niger*		*C. krusei*		*C. albican*	
	Zone of Inhibition (mm)							
	50 µg/ml	100 µg/ml	50 µg/ml	100 µg/ml	50 µg/ml	100 µg/ml	50 µg/ml	100 µg/ml
Quercetin	9±1.3	12±1.0	10±1.1	11±2.2	6±1.3	10±1.0	2±1.3	8±2.2
Citric acid	8±1.1	12±3.1	6±2.1	10±2.3	12±1.2	15±2.4	5±1.2	9±1.1
Q8SA	13±2.1	15±2.1	10±1.2	13±1.8	6±1.0	12±1.4	10±2.2	14±2.6
C1	17±2.1	22±2.2	10±1.1	13±2.1	15±2.1	18±2.3	20±1.1	23±2.4
C2	15±1.1	19±1.2	18±2.1	21±0.1	22±2.1	21±1.1	16±1.1	27±2.1
C3	25±1.3	28±2.1	22±1.1	27±1.2	22±1.4	26±1.2	20±1.1	21±1.1
C4	12±2.1	16±2.1	9±2.1	16±2.2	12±1.2	25±1.0	20±2.1	25±1.2

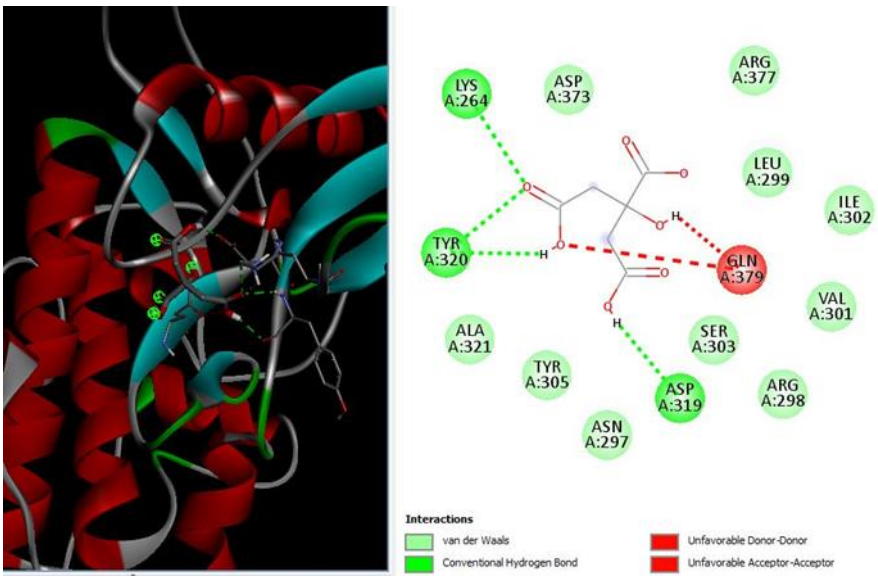

Appendix XI: 3D and 2D representation of the best interactions (-5.3 kcal/mol) of citric acid with 4COT

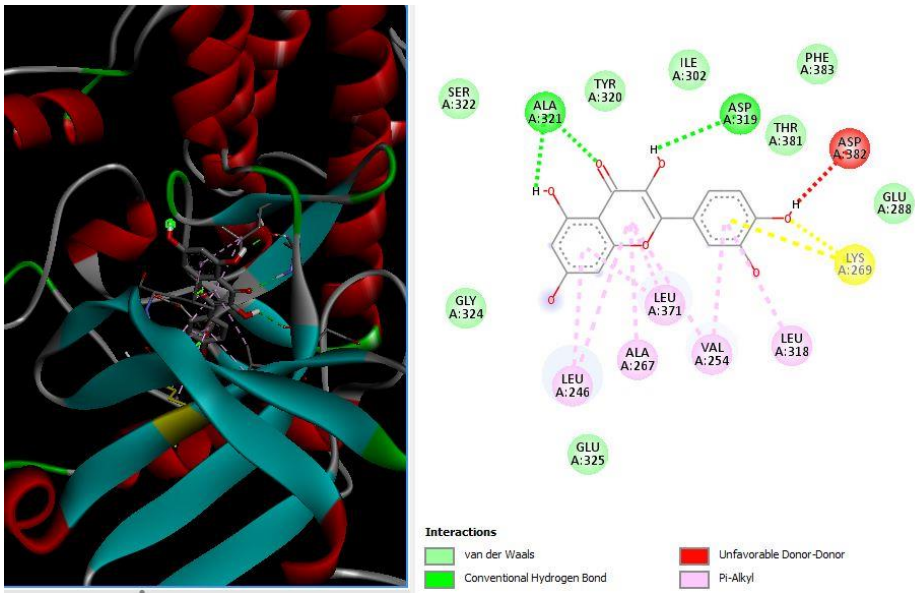

Appendix XII: 3D and 2D representation of the best interactions (-8.3 kcal/mol) of quercetin with 4COT

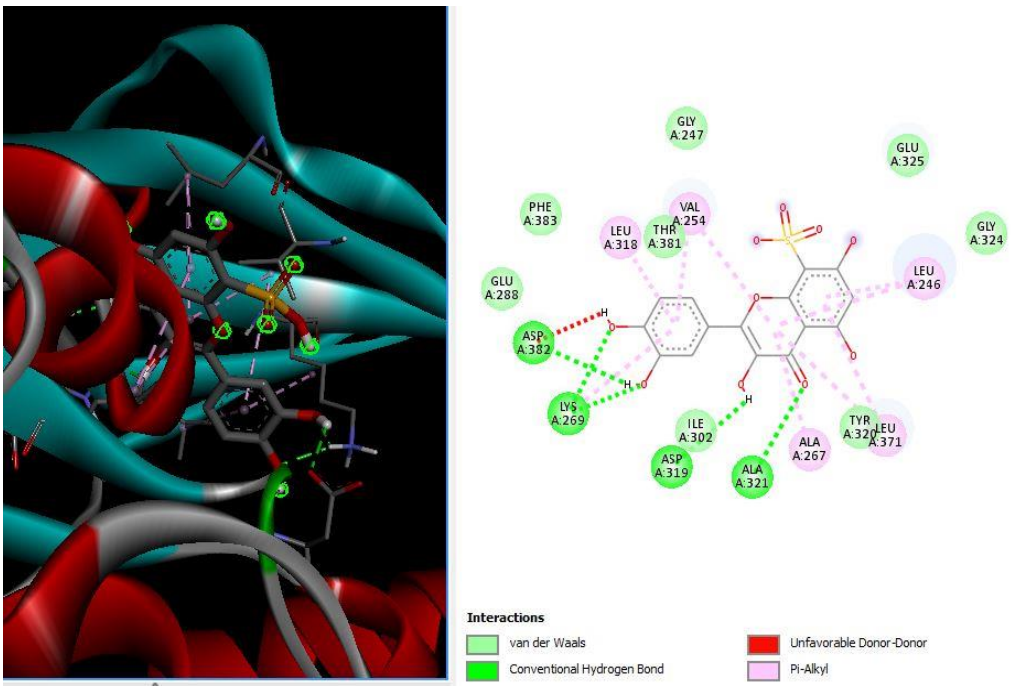

Appendix XIII: 3D and 2D representation of the best interactions (-8.3 kcal/mol) of Q8SA with 4COT

Appendix XIV: ADMET properties predictions of the ligands using pkCSM online software

Property	Model name	Q	Q8	CA
Absorption	Water solubility (log mol/L)	-3.18	-3.039	-0.428
Absorption	$CaCo_2$ permeability (log Papp in 10^{-6} cm/s)	-0.307	-0.424	-0.576
Absorption	Intestinal absorption (human) (% Absorbed)	74.634	41.043	0
Absorption	Skin Permeability (log Kp)	-2.735	-2.735	-2.735
Absorption	P-glycoprotein substrate(Yes/No)	Yes	Yes	Yes
Absorption	P-glycoprotein I inhibitor(Yes/No)	No	No	No
Absorption	P-glycoprotein II inhibitor(Yes/No)	No	No	No
Distribution	VDss (human) (log L/kg)	-0.05	0.101	-0.597
Distribution	Fraction unbound (human) (Fu)	0.132	0.184	0.503
Distribution	BBB permeability (log BB)	-1.481	-1.982	-1.219
Distribution	CNS permeability (log PS)	-3.383	-4.371	-3.62
Metabolism	CYP2D6 substrate(Yes/No)	No	No	No
Metabolism	CYP3A4 substrate(Yes/No)	No	No	No
Metabolism	CYP1A2 inhibitior(Yes/No)	Yes	No	No
Metabolism	CYP2C19 inhibitior(Yes/No)	No	No	No
Metabolism	CYP2C9 inhibitior(Yes/No)	No	No	No
Metabolism	CYP2D6 inhibitior(Yes/No)	No	No	No
Metabolism	CYP3A4 inhibitior(Yes/No)	Yes	No	No
Excretion	Total Clearance (log ml/min/kg)	0.547	0.747	0.902
Excretion	Renal OCT2 substrate(Yes/No)	No	No	No

Appendix XV: Toxicity predictions of the ligands using pkCSM online software

Property	Model name	Q	Q8	CA
Toxicity	AMES toxicity (Yes/No)	Yes	Yes	No
Toxicity	Max. tolerated dose (human) (log mg/kg/day)	0.951	0.818	1.633
Toxicity	hERG I inhibitor (Yes/No)	No	No	No
Toxicity	hERG II inhibitor (Yes/No)	No	No	No
Toxicity	Oral Rat Acute Toxicity (LD50) (mol/kg)	2.562	2.213	2.032
Toxicity	Oral Rat Chronic Toxicity (LOAEL) (log mg/kg_bw/day)	1.735	3.345	3.107
Toxicity	Hepatotoxicity (Yes/No)	No	No	No
Toxicity	Skin Sensitisation (Yes/No)	No	No	No
Toxicity	*T.Pyriformis* toxicity (log ug/L)	0.314	0.285	0.285
Toxicity	Minnow toxicity (log mM)	0.878	2.033	3.399

Appendix XVI: Predictions of some vital biochemical parameters of the ligands and the complexes using SwissADME and Protox-II online software

Parameters	Q	CA	Q8	C1	C2	C3	C4
LogS	-3.91	-0.54	-6.14	-6.59	-6.59	-6.59	-6.59
No. of H-bond Acceptors	7	7	10	17	17	17	17
No. of H-bond Donors	5	4	6	6	6	6	6
Concensus logP (average)	1.25	-1.51	0.83	-0.56	-0.55	-0.50	-0.59
Gastrointestinal Absorption	high	low	low	Low	low	low	Low
Lipinski Rule of 5(No of violations)	0	0	1	3	3	3	3
LD50 (mg/kg)	159		5000	600	500	600	500
Skin permeability (LogKp) cm/s	-7.06	-8.69	-7.80	-9.57	-9.58	-9.64	-9.51
Bioavailability score	0.35	0.56	0.11	0.11	0.11	0.11	0.11